

# Electron correlation effects in small iron clusters

G. Rollmann<sup>1</sup> and P. Entel

Theoretical Low-Temperature Physics,  
Physics Department, University of Duisburg-Essen, Campus 47048 Duisburg, Germany

Received 8 July, 2005; accepted in revised form 11 October, 2005

*Abstract:* We present results of first-principles calculations of structural, magnetic, and electronic properties of small Fe clusters. It is shown that, while the lowest-energy isomers of Fe<sub>3</sub> and Fe<sub>4</sub> obtained in the framework of density functional theory within the generalized gradient approximation (GGA) are characterized by Jahn-Teller-like distortions away from the most regular shapes (which is in agreement with other works), these distortions are reduced when electron correlation effects are considered explicitly as within the GGA+*U* approach. At the same time, the magnetic moments of the clusters are enhanced with respect to the pure GGA case, resulting in maximal moments (in the sense of Hund's rules) of 4  $\mu_B$  per atom for the ground state structures of Fe<sub>3</sub> and Fe<sub>4</sub>, and a total moment of 18  $\mu_B$  for Fe<sub>5</sub>. This already happens for moderate values of the Coulomb repulsion parameter  $U \sim 2.0$  eV and is explained by changes in the electronic structures of the clusters.

*Keywords:* Density functional theory, GGA + U, Fe cluster, Magnetic moment

*PACS:* 31.15.Ew, 36.40.Cg, 36.40.Mr

## 1 Introduction

Magnetic transition metal (TM) particles are an important ingredient in many state-of-the-art technological applications, ranging from catalysis to ultra-high density magnetic storage devices. In the latter case, miniaturization has already reached a point where particle sizes are so small that quantum effects start to play a role in determining their magnetic properties, which, in turn, show a pronounced size dependence. Therefore, a detailed understanding of the electronic structure of small TM clusters is not only very desirable from a fundamental point of view, but also inevitable if one wants to gain insight into the processes which govern particle formation necessary for the design of new materials with unique properties. One step towards this was taken a decade ago by Billas *et al.* who used a Stern-Gerlach type apparatus in combination with a time-of-flight mass spectrometer in order to measure magnetic moments of isolated TM clusters [1]. These experiments revealed that the magnetic moments of free Fe, Co, and Ni clusters are not just given by simple interpolations between the limiting values of the isolated atoms and the corresponding bulk materials, but rather change non-monotonically with cluster size in an oscillatory fashion. Unfortunately, resolution in cluster size (i.e., number of atoms) was only in the range of 10 %, and so a direct relation between cluster size and magnetic moment could not be established from these data.

<sup>1</sup>Corresponding author. E-mail: georg@thp.uni-duisburg.de

In the following years, numerous experimental studies have been undertaken to investigate different properties of small TM clusters. But while such measurements are relatively easy to perform for clusters deposited on surfaces (whose properties, though, can change drastically upon deposition due to their interaction with the substrate), the opposite is true for isolated clusters. This difficulty can be assigned to their great reactivity and the associated problem to produce particles with a given, well-defined size in high concentrations. Therefore, it may not seem surprising that, from experimental side, still not much is known about geometries, morphologies, and even magnetic properties of small TM clusters. In the case of Fe clusters, which are the subject of the present work, the bond length has only been measured for the dimer [2], and vibrational frequencies have been obtained for Fe<sub>2</sub> and Fe<sub>3</sub> [3]. While properties related to the electronic structure and energetics of the clusters have been obtained quite accurately [4, 5], again only sparse information is available regarding their magnetic moments.

On the other hand, due to the rapid development of computational capacities it has become possible to calculate properties of small atomic clusters from first principles with a high degree of accuracy in quantitative agreement with experiment. Therefore, in the case of Fe clusters, most information about structural and magnetic properties stems from such *ab initio* simulations, mainly based on density functional theory (DFT) [6]. For an overview, we refer to [7, 8] and references therein. It soon became clear, that it is important to go beyond the local density approximation (LDA) and include gradient corrections (GGA) when calculating the exchange and correlation energy. It also became evident that, in order to find the lowest-energy isomers for a given cluster size, it is important to allow for free relaxation of the atoms without imposing symmetry constraints. The reason for this is the presence of degenerate electronic states in highly symmetric clusters originating from the interaction of the *d*-manifold, giving rise to the Jahn-Teller effect [9], which in turn leads to distorted ground-state geometries with lower symmetry [10]. For Fe<sub>5</sub>, even a ground state characterized by a non-collinear magnetization density has been proposed [11]. But it could be shown that this is only a metastable state on the potential energy surface (PES) of the cluster, and that the energy can be lowered when the atoms are allowed to relax freely [12, 13].

Resulting from these different computational schemes, proposed magnetic moments reach from 8 to 10  $\mu_B$  for Fe<sub>3</sub>, 10 to 14  $\mu_B$  for Fe<sub>4</sub>, and 14 to 18  $\mu_B$  for Fe<sub>5</sub>, all related to different geometric arrangements of the atoms and different employed levels of theory [7,10-20]. Recently, two comprehensive investigations (in the framework of DFT) of the PES of Fe<sub>3</sub> and Fe<sub>4</sub> have revealed the true complexity of problem, yielding a high number of local minima close in energy [7]. In the case of the Fe trimer, at least 4 different states have been reported to be situated in a small energy range of less than 100 meV above the ground state. The situation is practically the same for Fe<sub>4</sub>, and therefore a definite assignment of the ground states has up to day neither been achieved for Fe<sub>3</sub> nor Fe<sub>4</sub>. Despite of this, the spin multiplicities were the same for all these low-lying states, giving rise to the assumption that the ground states of Fe<sub>3</sub> and Fe<sub>4</sub> have magnetic moments of 10 and 14  $\mu_B$ , respectively. By similar considerations one is lead to the conclusion that the lowest-energy isomer of Fe<sub>5</sub> possesses a total moment of 16  $\mu_B$  within DFT/GGA.

But even when all the aspects mentioned above are considered, a mayor drawback of current implementations of DFT remains in all these calculations: The well-known fact that, within conventional LDA (and also GGA), electron correlation due to intra-atomic Coulomb repulsion of localized *d* or *f* electrons is not described very well. Different methods have been proposed to overcome this limitation. Of these, the LDA + *U* method [21], where a Hubbard-like term *U* is incorporated into the density functional, has been applied successfully to a variety of problems in strongly correlated systems where ordinary LDA gives qualitatively wrong results. A prominent example are Mott insulators like the 3*d* TM oxides. In contrast to DFT in the LDA, which predicts metallic behavior or band gaps which are sometimes one order of magnitude too small, the insulating nature with correct band gaps is recovered within the LDA + *U* approach. For example,

for the case of an Fe-based system (antiferromagnetic  $\alpha$ -Fe<sub>2</sub>O<sub>3</sub>), we have shown that this method yields the correct high-pressure phase diagram [23].

Due to this lack in conventional LDA/GGA, one may challenge some of the results achieved for Fe clusters within DFT up to day. Add to that, recent high-level quantum-chemical calculations on the Fe dimer have given some indication that magnetic moments of small Fe clusters are actually larger than the values given above [24]. In this letter, we discuss the influence of electronic correlation on geometric and magnetic properties of small Fe clusters, by explicitly investigating the effect of the size of the parameter  $U$  on various properties of selected clusters. In the following section, we give a brief account on the employed computational scheme. Subsequently, we discuss our results for Fe<sub>3</sub>, Fe<sub>4</sub>, and Fe<sub>5</sub>. We conclude by making a prediction concerning the properties of larger clusters and give an outlook for future work.

## 2 Computational method

In our search for the lowest-energy isomers of Fe<sub>3</sub>, Fe<sub>4</sub>, and Fe<sub>5</sub>, we only have considered triangular geometries for Fe<sub>3</sub>, and three-dimensional structures for Fe<sub>4</sub> and Fe<sub>5</sub>, respectively, as these were found to be energetically most favorable in previous calculations. For each given arrangement of atoms in the cluster, the total energy was calculated in the framework of DFT [6] in combination with the GGA for the description of exchange and correlation in a functional form proposed by Perdew and Wang [25]. A number of 8 valence electrons was taken into account for each Fe atom, the remaining core electrons together with the nuclei were described by following the projector augmented wave method [26] as implemented in the Vienna *ab initio* simulation package [27]. The electronic wavefunctions were expanded in a plane-wave basis set with an energy cutoff of 335 eV. The clusters were positioned in cubic supercells of 11 Å length periodically repeated in space. The Brillouin zone integration was performed using the  $\Gamma$ -point only. We have allowed for a non-collinear magnetization density as described in [11].

For the GGA +  $U$  calculations, we have adopted a version proposed by Dudarev *et al.* [22]. In this implementation, the total energy depends on the difference  $U - J$ :

$$E_{\text{GGA}+U} = E_{\text{GGA}} + \frac{U - J}{2} \sum_{m\sigma} (n_{m\sigma} - n_{m\sigma}^2),$$

where  $n_{m\sigma}$  is the occupancy of the orbital with magnetic quantum number  $m$  and spin  $\sigma$ , and  $U$  and  $J$  represent the spherically averaged on-site Coulomb interaction and screened exchange integrals, respectively. It can be shown that within this formalism unoccupied  $d$  states are shifted towards higher energies by  $(U - J)/2$ , while the opposite is true for occupied  $d$  states. For a comprehensive discussion we refer to the literature [21, 22]. As the value of  $J$  was kept constant at  $J = 1$  eV in our calculations, the case  $U = 1$  eV corresponds here to the pure GGA limit, because in this case  $U - J = 0$  eV.

The structural relaxations were performed with the conjugate gradient method, without imposing any symmetry constraint. As initial structures, we have taken different lowest-energy states found in earlier calculations. The geometries were considered to be converged when all forces were smaller than 1 meV/Å. The distortions of the clusters are calculated with respect to a perfectly symmetric cluster with the same average bond length as explained in [12]. For the case of Fe<sub>3</sub> and Fe<sub>4</sub>, this simply reduces to the root-mean-square bond length fluctuation.

## 3 Results for Fe<sub>3</sub>

The energetic relationships for the Fe<sub>3</sub> cluster as obtained with different values for the parameter  $U$  are shown in Fig. 1. The spin multiplicities were varied from 9 to 13, yielding the differently

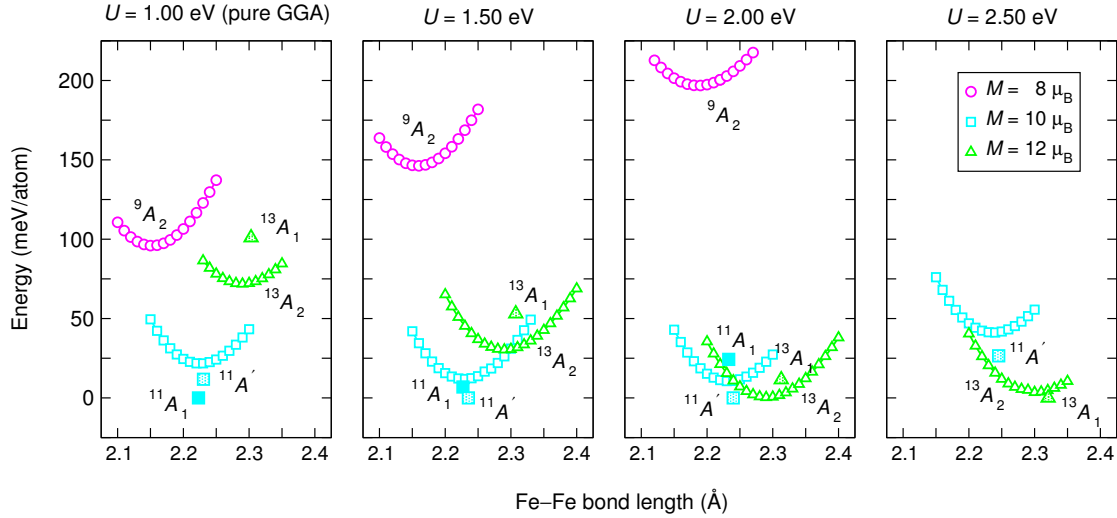


Figure 1: Relative total energy of the different isomers of the  $\text{Fe}_3$  cluster as a function of the average bond length, symmetry, and magnetic state for different values of  $U$ . The curves were shifted so that  $E = 0$  corresponds to the lowest-energy isomer found for a specific value of  $U$ . Open symbols refer to equilateral triangles, filled symbols denote energies of relaxed clusters.

colored curves. Open symbols correspond to equilateral triangular geometries with identical bond lengths ( $D_{3h}$  symmetry). For the relaxed clusters, whose energies are given by the filled symbols, the average interatomic distances were used for the Fe–Fe bond lengths.

In the case of conventional GGA ( $U = 1.00$  eV), we find that the lowest-energy states of  $\text{Fe}_3$  possess magnetic moments of  $10 \mu_B$ . When  $D_{3h}$  symmetry constraints are imposed, an energy minimum for an Fe–Fe bond length of  $2.225 \text{ \AA}$  is obtained. But this state is only metastable with respect to a Jahn-Teller distortion, as will be discussed below. When the atoms are allowed to relax freely, we find several states close in energy, of which the  $^{11}A_1$  state with one short and two longer bonds emerges as ground state. An  $^{11}A'$  state with  $C_s$  symmetry is located some  $12 \text{ meV/atom}$  higher in energy. A detailed discussion of the nature of these states (and also several others), including the influence of the employed GGA functionals, has been given elsewhere [7] and is beyond the scope of the present work. We only note that, although the individual bond lengths differ significantly from one isomer with  $10 \mu_B$  to the next, the average interatomic distances are nearly the same ( $\sim 2.23 \text{ \AA}$ ).

In contrast to the case of  $M = 10 \mu_B$ , equilateral triangles with spin multiplicities of 9 and 13 are stable with respect to structural deformations. But while the  $^9A_2$  state is the ground state in LDA calculations [7,10-11,15-19], it lies much higher in energy when GGA functionals are used. As can be seen from Fig. 1, the  $^9A_2$  state may only be lowest in energy for very small interatomic distances. Concerning isomers with a moment of  $12 \mu_B$ , we found a  $^{13}A_2$  state with identical bond lengths as well as a  $^{13}A_1$  state with one long ( $2.39 \text{ \AA}$ ) and two short ( $2.26 \text{ \AA}$ ) bonds. In the former state, two electrons occupy majority spin orbitals, which are higher in energy than empty minority spin orbitals (see Fig. 2), and therefore it is not a ground state for this arrangement of atoms and is irrelevant within DFT. The latter may be identified as the one found previously [7], but it does not play a role in the search for the lowest-energy isomer, as it is located well above in energy.

In spite of the different technical implementations, the results presented here are in very good agreement with those obtained in [7]. The small differences may be ascribed in part to our use of the PAW method compared to the all-electron calculations of the latter. Therefore, it may

Table 1: Structural and magnetic properties of selected isomers of  $\text{Fe}_3$  calculated within conventional GGA and GGA +  $U$  with different values for  $U$ . Magnetic moments are given in  $\mu_B$ , bond distances in  $\text{\AA}$ , distortions  $\delta$  in %, and energies in meV/atom.

$U$ (eV)	State	$M$	Symm.	$d_1$	$d_2$	$d_3$	$\delta$	E
1.00	$^{11}A_1$	10	$C_{2v}$	2.067	2.301	2.301	4.97	0
	$^{11}A'$	10	$C_s$	2.143	2.263	2.286	2.80	12
	$^{13}A_1$	12	$C_{2v}$	2.261	2.261	2.387	2.59	101
1.50	$^{11}A'$	10	$C_s$	2.149	2.251	2.306	2.91	0
	$^{11}A_1$	10	$C_{2v}$	2.069	2.306	2.306	5.01	7
	$^{13}A_1$	12	$C_{2v}$	2.262	2.262	2.398	2.77	53
2.00	$^{11}A'$	10	$C_s$	2.151	2.253	2.316	3.04	0
	$^{13}A_1$	12	$C_{2v}$	2.264	2.264	2.412	3.01	14
2.50	$^{13}A_1$	12	$C_{2v}$	2.266	2.266	2.431	3.35	0
	$^{11}A'$	10	$C_s$	2.152	2.257	2.327	3.21	27

be worthwhile to investigate the effect of including the Fe  $3p$  electrons to the valence electrons. However, first tests have already revealed that the results are qualitatively unchanged. On the other hand, we have used a plane-wave basis set, which is in the sense superior to localized orbitals that calculated quantities converge smoothly with the cutoff energy. We therefore assume that the major part of difference stems from the use of incomplete basis sets in [7].

When we increase the value of the Hubbard  $U$  parameter, we observe that the relative positions

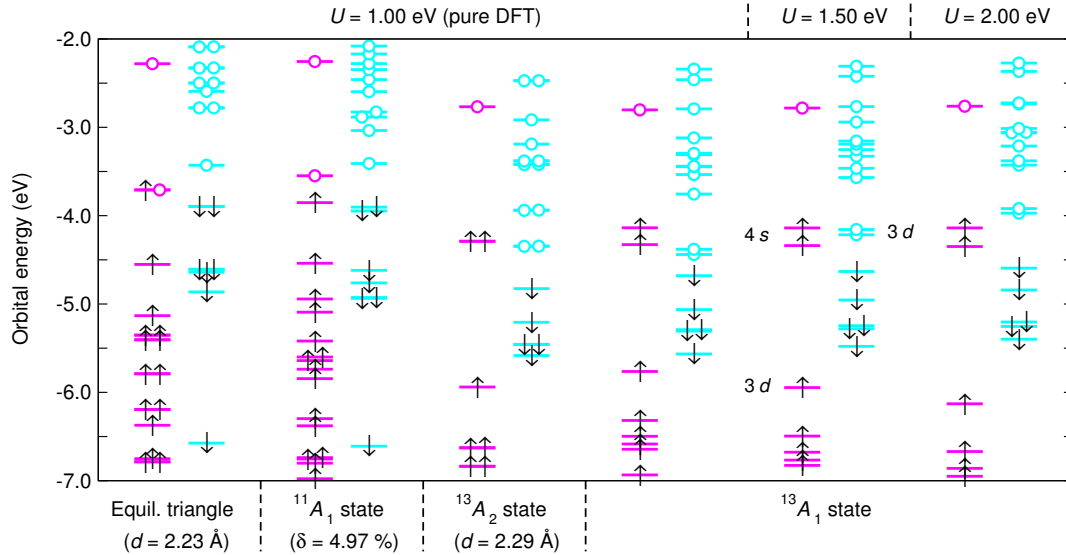


Figure 2: Kohn-Sham eigenvalues (horizontal bars) of selected states of the  $\text{Fe}_3$  cluster for conventional GGA and GGA +  $U$  with different values for  $U$ . Arrows represent electrons (of either spin), circles denote holes.

of the states are shifted. While the  ${}^9A_2$  state becomes energetically unfavorable, states with a total moment of  $12 \mu_B$  are lowered. At the same time, the order of  ${}^{11}A_1$  and  ${}^{11}A'$  are reversed, so that the latter becomes the lowest-energy isomer already for  $U = 1.50$  eV.

When  $U$  is increased to 2.00 eV, the isomers with multiplicities of 11 and 13 are getting practically degenerate, with  ${}^{11}A'$  still being the ground state. For  $U = 2.50$  eV, we finally encounter the  ${}^{13}A_1$  state, with a magnetic moment of  $12 \mu_B$  and a distortion of 3.4 %, being lowest in energy. We have listed structural and magnetic properties of selected isomers of  $Fe_3$  in Table 1.

In order to gain some insight into the mechanisms responsible for the ordering of states, we take a closer look at the electronic structures of the different isomers, but not without bearing in mind that in principle there is no direct physical meaning associated with the calculated one-electron orbitals in DFT. In Fig. 2 we have depicted these energy levels for several isomers and different values of  $U$ . As a starting point for the discussion we take the perfect triangle with a moment of  $10 \mu_B$ . We note that the highest occupied energy level is doubly degenerate, but occupied with only one electron. This immediately gives rise to a Jahn-Teller distortion leading to the  ${}^{11}A_1$  state, for which the degenerate levels split upon deformation of the cluster. Although the HOMO of  $Fe_3$  in the  ${}^{13}A_2$  is also twofold degenerate, there is no reason for a distortion due to the double occupation (promotion of one minority electron to the majority spin manifold). But because of the fact that two unoccupied minority  $3d$  orbitals are lower in energy than the occupied majority  $4s$  orbitals (violation of the aufbau principle), neither this state, nor the  ${}^{13}A_1$  state are ground states for this geometry and are in principle not accessible/relevant within DFT. But when the  $U$  parameter is increased, this situation changes. We observe, that occupied majority spin  $d$  states are shifted towards lower energies, while the empty minority spin  $d$  states are moved upwards. This leads to a state crossing at the Fermi energy for  $U \sim 1.50$  eV and to the fact that, from around  $U = 2.00$  eV, the aufbau principle is fulfilled and the  ${}^{13}A_1$  is the ground state. As we saw above, it is even the global energy minimum of the  $Fe_3$  cluster for  $U = 2.50$  eV.

## 4 Results for $Fe_4$ and $Fe_5$

The energetic relationships for the  $Fe_4$  cluster are depicted in Fig. 2. We again begin our discussion with the situation within conventional GGA. When tetrahedral symmetry constraints are imposed, the energy is minimal for a cluster with a magnetic moment of  $12 \mu_B$  and interatomic distances of 2.276 Å. This state has been found in previous studies. Ballone and Jones were the first to show that the energy can be lowered when symmetry is broken. They found a state with  $D_{2d}$  symmetry (butterfly structure) by molecular dynamics simulations. In our calculation, this isomer (filled circle) has 2 short and 4 longer bonds of 2.20 and 2.32 Å, respectively. Although the lowest-energy isomer of  $Fe_4$  (found within DFT/GGA) belongs to the same point group, it is characterized by a magnetic moment of  $14 \mu_B$ , 2 long and 4 shorter bonds of 2.54 and 2.23 Å. As in the case of  $Fe_3$ , there are again several minima found within a small energy range, and for a more comprehensive discussion we refer to [7].

When we increase the value for the Hubbard  $U$ , we first observe a similar effect as in the case of the Fe trimer. Low-moment states shifted to higher energies, and the isomers with a moment of  $16 \mu_B$  are becoming favorable. But, while in the case of  $Fe_3$  the overall situation had not yet changed for  $U = 1.50$  eV, we here get already the high-moment state lowest in energy among all perfect tetrahedra. For a value of  $U = 2.00$  eV, also the lowest-energy isomer of  $Fe_4$  carries a moment of  $16 \mu_B$  or  $4 \mu_B$  per atom.

A further discussion of the different states will not be given here. Instead, we would like to finish our remarks by presenting a result for the  $Fe_5$  cluster. It turns out that, while the ground state found within conventional DFT has a multiplicity of 17, this value is increased to 19 already for  $U = 1.50$  eV. The associated distortion of the cluster is reduced from 4.6 to 3.0%.

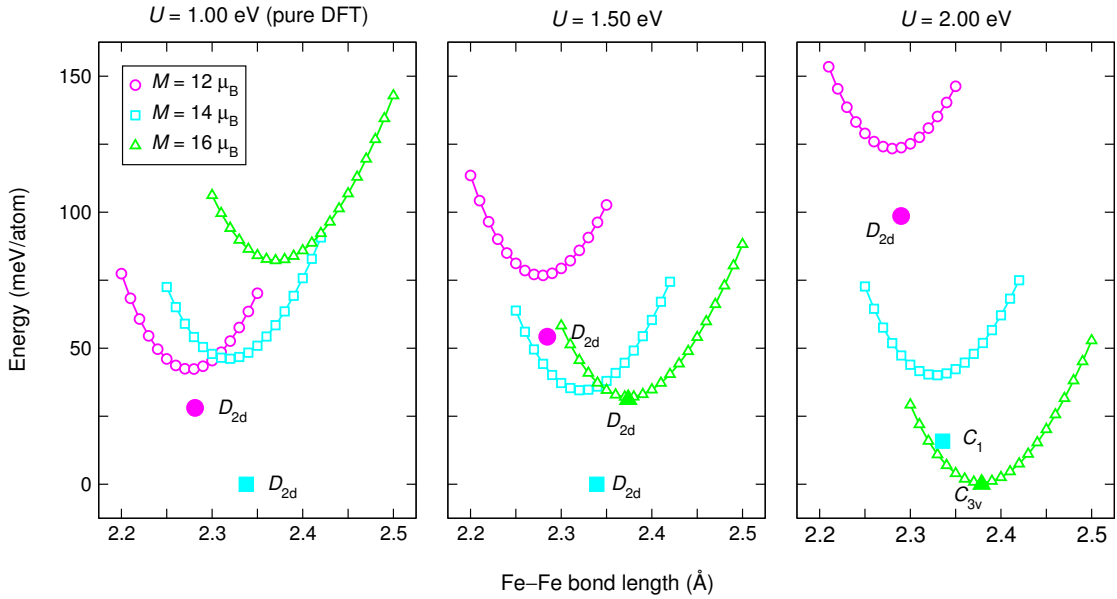


Figure 3: Total energy of the  $\text{Fe}_4$  cluster as a function of cluster size, symmetry, and total magnetic moment for different values of  $U$ . The curves were shifted so that  $E = 0$  corresponds to the lowest-energy isomer found for a specific value of  $U$ . Open symbols refer to perfect tetrahedral cluster, filled symbols denote energies of relaxed clusters.

## 5 Conclusion

We have shown that the order of states of small Fe clusters (namely,  $\text{Fe}_3$  and  $\text{Fe}_4$ ) changes drastically compared to conventional GGA when electronic correlation effects are considered explicitly. Total magnetic moments of the lowest-energy isomers are by  $2 \mu_B$  higher, yielding values of  $12$  and  $16 \mu_B$  for  $\text{Fe}_3$  and  $\text{Fe}_4$ , respectively. This was explained to be due to the shift of one-electron Kohn-Sham levels which depends on the magnitude of  $U$ . While the situation is not so clear for the trimer, where even for  $U = 2$  eV no definite assignment of the ground state could be made, the lowest-energy isomer of  $\text{Fe}_4$  was found to be a nearly perfect tetrahedron with a total moment of  $16 \mu_B$  already for  $U = 2$  eV. A similar behavior was encountered for  $\text{Fe}_5$ . We expect this trend observed for the small clusters to continue as the number of atoms is increased, and therefore predict the calculated moments of larger Fe clusters to be higher (by at least  $2 \mu_B$ ) when electron correlation is explicitly taken into account. In order to justify reasonable choices of  $U$ , we emphasize that it is inevitable to perform further investigations of other properties related to the electronic structure of these clusters, like ionization potentials, electron affinities, and binding energies, as these have been obtained in part to good accuracy in experiments.

## Acknowledgment

This work has been supported by the German Science Foundation through the SFB 445 “*Nano-Particles from the Gasphase: Formation, Structure, Properties*”. The calculations have been performed at the Regional Computer Center of the University of Cologne (RRZK).

## References

- [1] I.M.L. Billas, J.A. Becker, A. Châtelain, and W. A. de Heer, Magnetic moments of iron clusters with 25 to 700 atoms and their dependence on temperature, *Phys. Rev. Lett.* **71** 4067-4070(1993).  
I.M.L. Billas, A. Châtelain, and W.A. de Heer, Magnetism of Fe, Co and Ni clusters in molecular beams, *J. Magn. Magn. Mater.* **168** 64-84(1997).
- [2] P.A. Montano and G.K. Shenoy, EXAFS study of iron monomers and dimers isolated in solid argon, *Solid State Commun.* **35** 53-56(1980).  
H. Purdum, P.A. Montano, and G.K. Shenoy, Extended x-ray-absorption-fine-structure study of small Fe molecules isolated in solid neon, *Phys. Rev. B* **25** 4412-4417(1982).
- [3] M. Moskovits and D.P. DiLella, Di-iron and nickeliron, *J. Chem. Phys.* **73** 4917-4924(1980).  
T.L. Haslett, K.A. Bosnick, S. Fedrigo, and M. Moskovits, Resonance Raman spectroscopy of matrix-isolated mass-selected Fe<sub>3</sub> and Ag<sub>3</sub>, *J. Chem. Phys.* **111** 6456-6461(1999).
- [4] D.G. Leopold and W.C. Lineberger, A study of the low-lying electronic states of Fe<sub>2</sub> and Co<sub>2</sub> by negative ion photoelectron spectroscopy, *J. Chem. Phys.* **85** 51-55(1986).  
D.G. Leopold, J. Almlöf, W.C. Lineberger, and P.E. Taylor, A simple interpretation of the Fe<sub>2</sub><sup>-</sup> photoelectron spectrum, *J. Chem. Phys.* **88** 3780-3783(1988).
- [5] E.A. Rohlfing, D.M. Cox, A. Kaldor, and K.H. Johnson, Photoionization spectra and electronic structure of small iron clusters, *J. Chem. Phys.* **81** 3846-3851(1984).  
E.K. Parks, T.D. Klots, and S.L. Riley, Chemical probes of metal cluster ionization potentials, *J. Chem. Phys.* **92** 3813-3826(1990).  
S. Yang and M.B. Knickelbein, Photoionization studies of transition metal clusters: Ionization potentials for Fe<sub>n</sub> and Co<sub>n</sub>, *J. Chem. Phys.* **93** 1533-1539(1990).  
L.S. Wang, H.S. Cheng, and J. Fan, Photoelectron spectroscopy of size-selected transition metal clusters: Fe<sub>n</sub><sup>-</sup>,  $n = 3 - 24$ , *J. Chem. Phys.* **102** 9480-9493(1995).  
L.S. Wang, X. Li, and H.F. Zhang, Probing the electronic structure of iron clusters using photoelectron spectroscopy, *Chem. Phys.* **262** 53-63(2000).
- [6] P. Hohenberg and W. Kohn, Inhomogeneous electron gas, *Phys. Rev.* **136** B864-B871(1964).  
W. Kohn and L.J. Sham, Self-consistent equations including exchange and correlation effects *Phys. Rev.* **140** A1133-A1138(1965).
- [7] S. Chrétien and D.R. Salahub, Kohn-Sham density-functional study of low-lying states of the iron clusters Fe<sub>n</sub><sup>+</sup>/Fe<sub>n</sub>/Fe<sub>n</sub><sup>-</sup> ( $n = 1 - 4$ ), *Phys. Rev. B* **66** 155425(2003).  
G.L. Gutsev and C.W. Bauschlicher, Jr., Electron affinities, ionization energies, and fragmentation energies of Fe<sub>n</sub> Clusters ( $n = 2 - 6$ ): A density functional theory study, *J. Phys. Chem. A* **107** 7013-7023(2003).
- [8] G. Rollmann, S. Sahoo, and P. Entel, Structure and magnetism in iron clusters (Eds: S.N. Sahu and P.K. Choudhury), *Proc. Indo-US Workshop "Nanoscale Materials: From Science to Technology"*, Nova Science, New York, 2005, in print.
- [9] H.A. Jahn and E. Teller, Stability of polyatomic molecules in degenerate electronic states. I. Orbital degeneracy, *Proc. Roy. Soc. (London)* **A161** 220-235(1937).
- [10] M. Castro, The role of the Jahn-Teller distortions on the structural, binding, and magnetic properties of small Fe<sub>n</sub> clusters,  $n \leq 7$ , *Int. J. Quantum Chem.* **64** 223-230(1997).

- [11] D. Hobbs, G. Kresse, and J. Hafner, Fully unconstrained noncollinear magnetism within the projector augmented-wave method, *Phys. Rev. B* **62** 11556-11570(2000).
- [12] G. Rollmann, S. Sahoo, and P. Entel, Structural and magnetic properties of Fe-Ni clusters, *Phys. Status Solidi A* **201** 3263-3270(2004).
- [13] G. Rollmann, P. Entel, and S.Sahoo, Competing structural and magnetic effects in small iron clusters, *Comput. Mater. Sci.* (2005), in print.
- [14] H. Tatewaki, M. Tomonari, and T. Nakamura, The band structure of small iron clusters from Fe<sub>1</sub> to Fe<sub>6</sub>, *J. Chem. Phys.* **88** 6419-6430(1988).
- [15] M. Castro and D.R. Salahub, Density-functional calculations for small iron clusters: Fe<sub>n</sub>, Fe<sub>n</sub><sup>+</sup>, and Fe<sub>n</sub><sup>-</sup> for n ≤ 5, *Phys. Rev. B* **49** 11842-11852(1994).
- [16] P. Ballone and R.O. Jones, Structure and spin in small iron clusters, *Chem. Phys. Lett.* **233** 632-638(1995).
- [17] M. Castro, C. Jamorski, and D.R. Salahub, Structure, bonding, and magnetism of small Fe<sub>n</sub>, Co<sub>n</sub>, and Ni<sub>n</sub> clusters, n ≤ 5, *Chem. Phys. Lett.* **271** 133-142(1997).
- [18] T. Oda, A. Pasquarello, and R. Car, Fully unconstrained approach to noncollinear magnetism: application to small Fe clusters, *Phys. Rev. Lett.* **80** 3622-3625(1998).
- [19] O. Diéguez *et al.*, Density-functional calculations of the structures, binding energies, and magnetic moments of Fe clusters with 2 to 17 atoms, *Phys. Rev. B* **63** 205407(2001).
- [20] Ž. Šljivančanin and A. Pasquarello, Supported Fe nanoclusters: evolution of magnetic properties with cluster size, *Phys. Rev. Lett.* **90** 247202(2003).
- [21] V.I. Anisimov, J. Zaanen, and O.K. Andersen, Band theory and Mott insulators: Hubbard U instead of Stoner I, *Phys. Rev. B* **44** 943-954(1991).
- [22] S.L. Dudarev, G.A. Botton, and S.Y. Savrasov, C.J. Humphreys, and A.P. Sutton, Electron-energy-loss spectra and the structural stability of nickel oxide: An LSDA+U study, *Phys. Rev. B* **57** 1505-1509(1998).
- [23] G. Rollmann, A. Rohrbach, P. Entel, and J. Hafner, First-principles calculation of the structure and magnetic phases of hematite, *Phys. Rev. B* **69** 165107(2004).
- [24] O. Hübner and J. Sauer, Confirmation of <sup>9</sup>Σ<sub>g</sub><sup>-</sup> and <sup>8</sup>Σ<sub>u</sub><sup>-</sup> ground states of Fe<sub>2</sub> and Fe<sub>2</sub><sup>-</sup> by CASSCF/MRCI, *Chem. Phys. Lett.* **358** 442-448(2002).  
C. W. Bauschlicher, Jr. and A. Ricca, Can all of the Fe<sub>2</sub> experimental results be explained?, *Mol. Phys.* **101** 93-98(2003).
- [25] J.P. Perdew and Y. Wang, Accurate and simple analytic representation of the electron-gas correlation energy, *Phys. Rev. B* **45** 13244-13249(1992).
- [26] P.E. Blöchl, Projector augmented-wave method, *Phys. Rev. B* **50** 17953-17979(1994).  
G. Kresse and D. Joubert, From ultrasoft pseudopotentials to the projector augmented-wave method, *Phys. Rev. B* **59** 1758-1775(1999).
- [27] G. Kresse and J. Furthmüller, Efficient iterative schemes for *ab initio* total-energy calculations using a plane wave basis set, *Phys. Rev. B* **54** 11169-11186(1996).  
G. Kresse and J. Furthmüller, Efficiency of ab-initio total energy calculations for metals and semiconductors using a plane-wave basis set, *Comput. Mater. Sci.* **6** 15-50(1996).